ARTICLE

ACS chemical biology

HaloTag: A Novel Protein Labeling Technology for Cell Imaging and Protein Analysis

Georgyi V. Los[†,*], Lance P. Encell[†], Mark G. McDougall[‡], Danette D. Hartzell[†], Natasha Karassina[†], Chad Zimprich[†], Monika G. Wood[†], Randy Learish[†], Rachel Friedman Ohana[†], Marjeta Urh[†], Dan Simpson[†], Jacqui Mendez[†], Kris Zimmerman[†], Paul Otto[†], Gediminas Vidugiris[†], Ji Zhu[‡], Aldis Darzins[†,§], Dieter H. Klaubert[‡], Robert F. Bulleit[†], and Keith V. Wood[†]

[†]Promega Corporation, 2800 Woods Hollow Rd., Madison, Wisconsin 53711 and [‡]Promega Biosciences Incorporated, 277 Granada Dr., San Luis Obispo, California 93401, [§]Present address: National Renewable Energy Laboratory, 1617 Cole Blvd., Golden, Colorado 80401

ABSTRACT We have designed a modular protein tagging system that allows different functionalities to be linked onto a single genetic fusion, either in solution, in living cells, or in chemically fixed cells. The protein tag (HaloTag) is a modified haloalkane dehalogenase designed to covalently bind to synthetic ligands (HaloTag ligands). The synthetic ligands comprise a chloroalkane linker attached to a variety of useful molecules, such as fluorescent dyes, affinity handles, or solid surfaces. Covalent bond formation between the protein tag and the chloroalkane linker is highly specific, occurs rapidly under physiological conditions, and is essentially irreversible. We demonstrate the utility of this system for cellular imaging and protein immobilization by analyzing multiple molecular processes associated with NF-κB-mediated cellular physiology, including imaging of subcellular protein translocation and capture of protein−protein and protein−DNA complexes.

As a result of the complexity inherent in cellular processes, multiple analytical methods are generally required to clearly elucidate their underlying mechanisms. Many of these methods rely on the ability to specifically tag proteins through the creation of genetic fusions, thereby imparting unique properties for selective protein visualization, capture, and manipulation within biochemically complex environments. Fluorescent proteins in particular, such as GFP, have been useful for studying protein behavior in living cells (recently reviewed in refs 1 and 2). As fusion tags, fluorescent proteins have served as markers for protein localization, translocation, interactions, and conformational change. Other fusion tags, such as His tag and FLAG tag, allow for the protein capture and purification (*3, 4*). Although each tag provides useful functionalities, any single tag is limited with respect to its range of capabilities. Thus, studies involving multiple analytical methods often require the use of more than one tag and therefore multiple genetic constructions.

It may be more efficient to use a single tag that could be readily reconfigured to meet the needs of different experimental tasks. This approach could also facilitate data correlation across a series of related experiments. Strategies for rapidly attaching chemical functionalities onto a protein tag have been offered, relying on synthetic molecules designed to selectively interact with particular proteins or polypeptides (recently reviewed in refs 5–8). The intention is to combine the specificity afforded by a genetically encoded protein tag with the functional diversity enabled by synthetic chemistry, allowing the incorporation of a wide range of fluorescent labels, affinity handles, or solid supports. Although this

***Corresponding author, georgyi.los@promega.com.**

Received for review January 30, 2008 and accepted May 5, 2008.

Published online June 6, 2008

10.1021/cb800025k CCC: $40.75

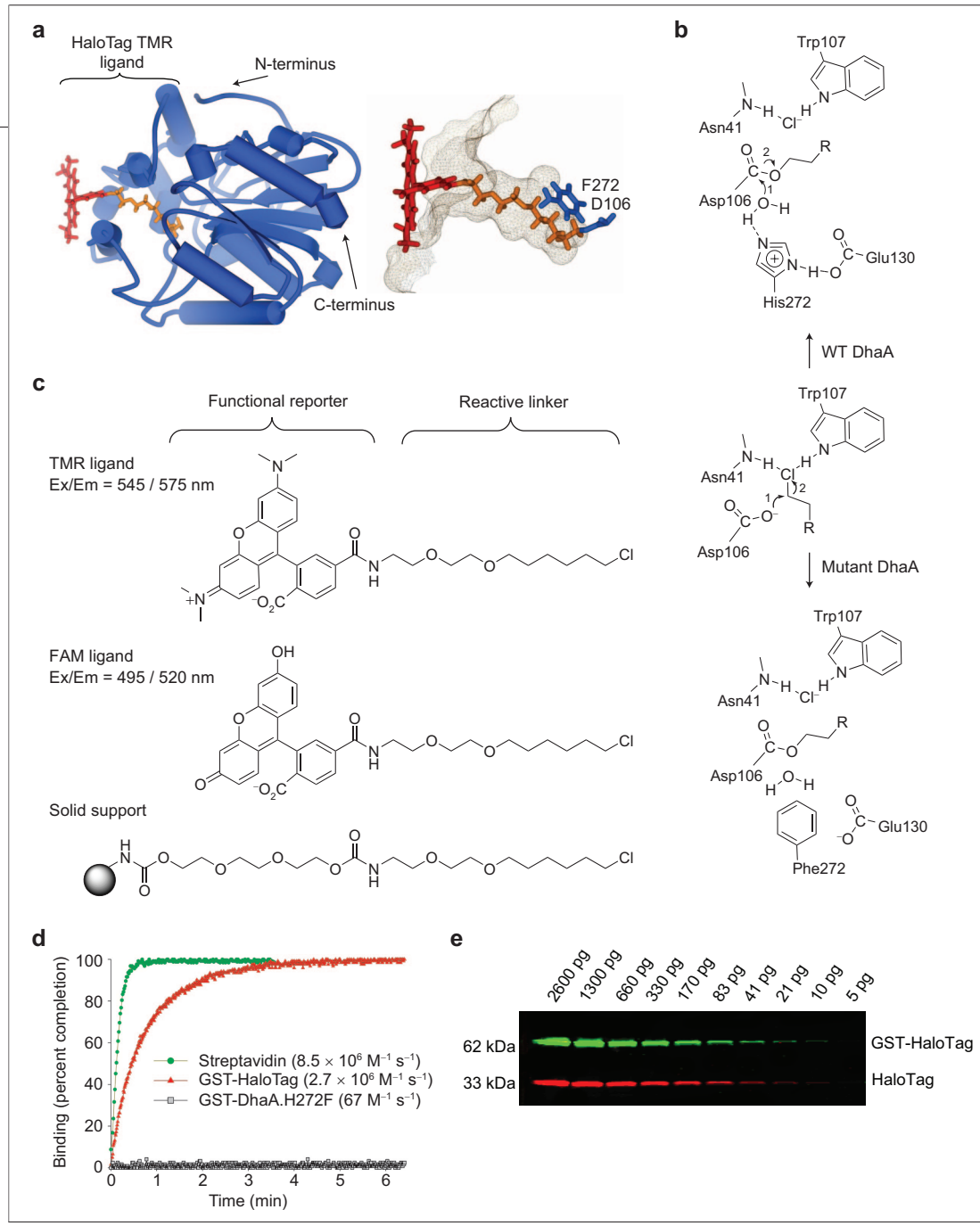

Figure 1. Overview of the HaloTag system. a) The HaloTag protein (model) and close-up of the ligand tunnel (outlined by a mesh Connolly surface) with covalently bound TMR ligand. b) Reaction mechanism of wild-type (WT) and mutant dehalogenase. Nucleophilic displacement of the terminal chloride with Asp106 leads to a covalent alkyl-enzyme intermediate. In the wild-type enzyme, His272 acts as a general base to catalyze hydrolysis of the intermediate, resulting in product release and regeneration of enzyme. In the mutant protein, the substituted Phe272 is ineffective as a base, thereby trapping the reaction intermediate as a stable covalent adduct. c) Structure of fluorescent ligands (TMR and FAM) and agarose surface (HaloLink Resin). d) Labeling kinetics (TMR ligand) compared to streptavidin-biotin and DhaA.H272F. Reactions between 10 nM protein and 2.5 nM ligand at 25 °C were monitored over time by fluorescence polarization. Apparent second-order rate constants shown for GST-HaloTag and streptavidin were calculated using this data, whereas the rate constant for GST-DhaA.H272F was calculated from a reaction between 15 μM protein and 15 nM ligand (data not shown). The calculated binding rate for streptavidin-biotin is consistent with previously reported values (*17*). e) Fluorescence imaging of labeled HaloTag (red) and GST-HaloTag (green) in denaturing protein electrophoresis. One microgram of purified HaloTag or GST-HaloTag was labeled with the TMR (red) or FAM (green) ligand, respectively (1 μM; 15 min; RT). The reaction mixtures were combined, incubated for an additional 60 min, and then resolved by SDS-PAGE.

approach can be effective, it may be limited by concerns over reversibility of the chemical attachment (*9*), cellular toxicity (*9, 10*), and labeling specificity in mammalian systems (*11, 12*).

We have employed a novel approach for creating a modular protein tag using a modified bacterial haloalkane dehalogenase (EC 3.8.1.5) designed to form a covalent bond with synthetic ligands (Figure 1, panel a). Haloalkane dehalogenases remove halides from aliphatic hydrocarbons by a nucleophilic displacement mechanism (*13*). A covalent ester bond is formed during catalysis between an aspartate in the enzyme and the hydrocarbon substrate. Base-catalyzed hydrolysis of this covalent intermediate subsequently releases the hydrocarbon as an alcohol and regenerates the aspartate nucleophile for additional rounds of catalysis (Figure 1, panel b). The based-catalyzed cleavage is mediated by a conserved histidine located near the aspartate nucleophile. It was previously shown with dehalogenase from *Xanthobacter* (DhlA) that mutating this histidine led to the formation of a stable bond with 1,2-dibromoethane (*14*). By applying an analogous mutation to the more promiscuous *Rhodococcus* dehalogenase (DhaA), we show that stable bonds can be readily made with synthetic molecules appended to a chloroalkane linker, thus allowing easy linkage to a range of functionalities.

Trapping the covalent intermediate enables irreversible attachment of the chemical functionalities and the dehalogenase structure provides reaction specificity and efficiency. Bacterial dehalogenases are relatively small and by utilizing an enzymatic reaction foreign to mammalian cells, cross-reactive interference is negligible with the endogenous mammalian biochemistry. Furthermore, the synthetic ligands can be designed for compatibility with mammalian cell culture and permeability to cellular membranes. The resulting technology, called HaloTag, thus allows specific fluorescent labeling of fusion proteins in both living or chemically fixed cells and irreversible capture of these proteins onto solid supports.

To demonstrate the utility of our approach, we show how a single genetic fusion can be utilized in multiple analytical methods for characterizing intracellular signaling by the nuclear factor (NF)-κB. NF-κB plays an important role in inflammation, autoimmune response, and apoptosis by regulating the expression of genes involved in these processes (for a recent review see ref 15). We show that by using the HaloTag protein and a set of alternative chloroalkane ligands (*e.g.*, fluorescent carboxytetramethylrhodamine (TMR) ligand and chloroalkane-functionalized agarose beads) we can analyze subcellular localization, translocation, and degradation of NF-κB proteins (p65 and IκB). Moreover, using the same fusion protein, we were able to correlate the translocation dynamics of p65 with formation of the p65/p50/IκB protein complex and binding of p65 to the IκB promoter.

RESULTS AND DISCUSSION

Development of HaloTag System Components. Creating the modular protein tag required developing both a modified protein capable of bonding efficiently with haloalkanes and an optimal chloroalkane linker for attaching onto synthetic molecules. The crystal structure of DhaA shows that the catalytic amino acids are located in a deep pocket, 15 Å from the protein surface (*16*). The α-methylene chloride of the linker must be properly positioned relative to the nucleophilic Asp^{106} in order to form a covalent adduct with DhaA. Because relatively large functional groups attached to the chloroalkane (*e.g.*, fluorophores) might prevent the chloroalkane from reaching the catalytic site of the enzyme, the length of the linker may be critical for bond formation. Therefore, several linkers needed to be designed and tested for reactivity with DhaA. Reactivity was determined using a pH-indicator-based assay for detecting halide release applied to an affinity purified GST-DhaA fusion protein (see Supporting Information).

Appended onto carboxyfluorescein (FAM), we achieved efficient halide release when the linker was 14 atoms long and contained 6 carbon atoms proximal to the terminal chlorine (Figure 1, panel c). This linker was incorporated in all subsequent HaloTag ligands, including HaloLink surfaces. Ligands intended for intracellular labeling were further designed for permeability in mammalian cells and to have no toxicity or effect on cellular morphology (Supplementary Figure 1). An additional spacer was included for agarose beads to move the reactive chlorine further from the surface (Figure 1, panel c).

To develop a DhaA variant capable of stably binding with the HaloTag ligands, four mutant proteins were created having the catalytic His^{272} residue substituted with Gln, Gly, Ala, or Phe. Upon expression as GST fusions in *E. coli*, only the Phe mutant (DhaA.H272F) pro-

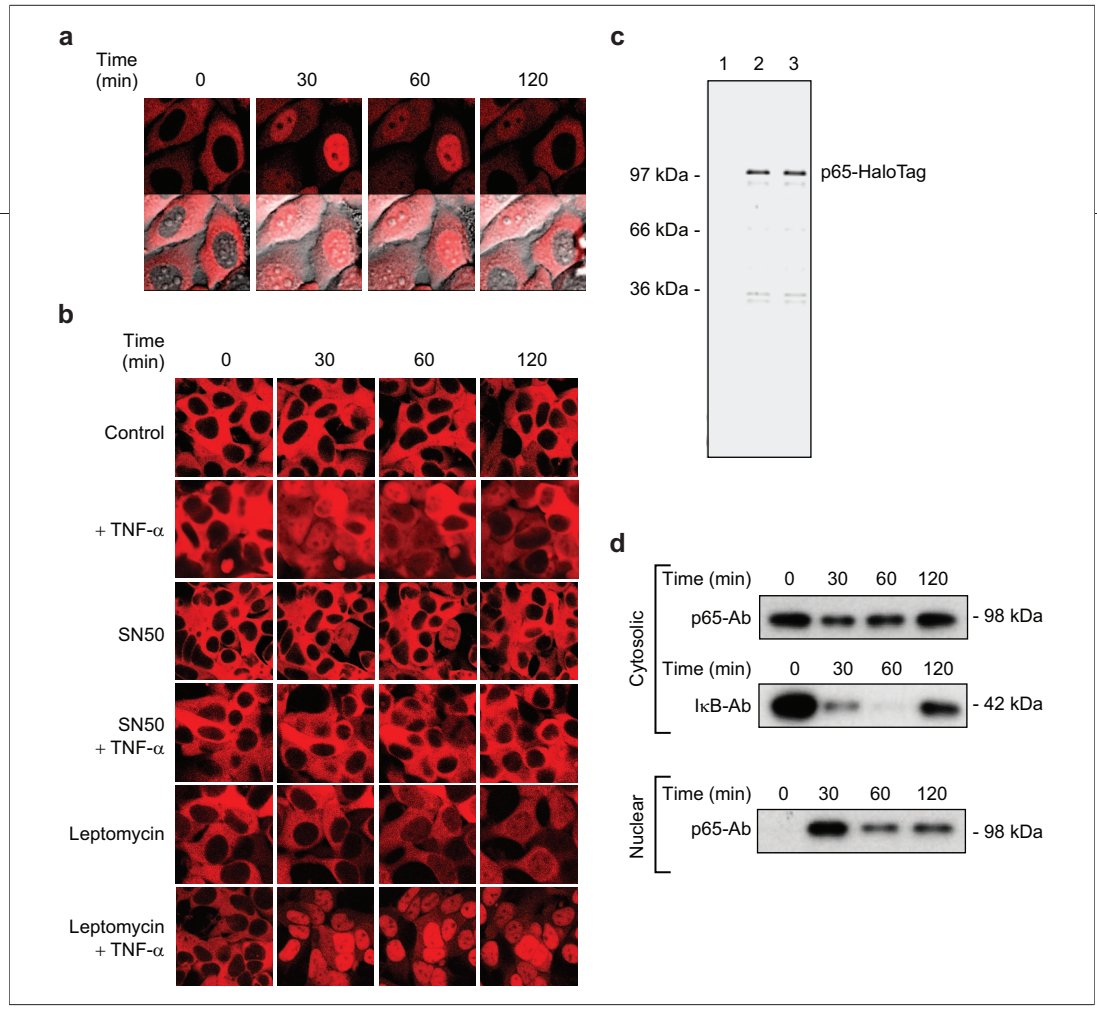

Figure 2. Nuclear translocation of p65-HaloTag in response to TNF-α stimulation. a) Time series of images showing HeLa cells transiently expressing p65-HaloTag fusion protein, labeled with the TMR ligand (5 μM; 15 min; 37 °C) and treated with TNF-α (10 ng mL^{-1}). b) Time series of images showing HEK-293 cells stably expressing p65-HaloTag fusion protein and labeled with the TMR ligand, with or without stimulation by TNF-α (10 ng mL^{-1}). Images were taken every 10 min for 3 h (images shown for 0, 30, 60, and 120 min after stimulation). Inhibition of nuclear accumulation of p65-HaloTag was observed in cells treated with 18 μM SN50 for 15 min prior to addition of TNF-α. Nuclear accumulation of p65-HaloTag was enhanced in cells treated with 50 μM leptomycin B for 30 min prior to addition of TNF-α. c) Fluorescence image of lysates from HeLa cell expressing p65-HaloTag fusion protein and labeled with the TMR ligand. The cells were mock transfected (lane 1) or transiently transfected with vector encoding the fusion protein (lanes 2 and 3) and labeled with the TMR ligand (5 μM; 37 °C) for15 min (lanes 1 and 2) or 60 min (lane 3). The cells were then lysed and proteins resolved by SDS-PAGE. d) Western blot analysis showing TNF-α-dependent nuclear translocation of p65-HaloTag fusion protein and degradation of IκB. Cells in 24-well plates were treated with TNF-α (10 ng mL^{-1}) for the indicated times. Following separation of cytosolic and nuclear fractions, proteins were resolved by SDS-PAGE and visualized using anti-p65 or anti-IκB antibodies.

duced high levels of soluble protein (data not shown). In contrast to DhaA, this mutant did not exhibit enzymatic activity as determined by the pH-indicator assay following incubation with the FAM ligand (Supplementary Figure 2). In a separate experiment, DhaA.H272F combined with the TMR ligand yielded a fluorescent adduct that was stable under the denaturing conditions used for SDS-PAGE analysis (0.1% SDS; 95 °C; 5 min). No fluorescent labeling of unmodified DhaA was detected under the same conditions (Supplementary Figure 3). Formation of a stable covalent bond between DhaA.H272F and the FAM ligand was evident also by MALDI-TOF analysis (data not shown). Using fluorescence polarization applied to purified GST-DhaA.H272F, apparent second-order rate constants for the FAM and TMR ligands were determined to be 3 and 67 M^{-1} s^{-1}, respectively (Figure 1, panel d).

These apparent binding rates are low compared to those of common affinity-based interactions like biotin-streptavidin, potentially hampering the practical utility of DhaA.H272F (*17*). To overcome this, we used a "semi-rational" strategy, incorporating protein−ligand modeling, site-saturation mutagenesis, and a high-throughput screen for faster binding kinetics. Several variants were identified with dramatically improved binding rates. The best of these, DhaA.H272F with K175M/C176G/Y273L

substitutions (HaloTag), had an apparent second-order rate constant of $2.7 \times 10^6\ M^{-1}\ s^{-1}$ for the TMR ligand, comparable to the calculated binding rate for tetrameric streptavidin with TMR-biotin (Figure 1, panel d). These kinetics are over 4 orders of magnitude above that of the DhaA.H272F parent, thus allowing the reaction to reach completion even under low concentrations of ligand. This may be particularly important for intracellular applications, where differential diffusion of the ligand could result in uneven distribution within the cells.

Irreversibility of the covalent bond was shown by separately labeling purified HaloTag protein and GST-HaloTag fusion protein with an excess of the TMR and FAM ligands respectively (1 μM; 15 min; RT), followed by further incubation with the two samples combined (60 min; RT). Resolving by SDS-PAGE revealed two fluorescent protein bands, distinctly labeled with the respective HaloTag ligands and without any evidence of cross-labeling (Figure 1, panel e). This indicates that labeling was completed before the reactions were combined and that bound ligand could not exchange with the excess free ligand.

Imaging of Mammalian Cells Expressing p65-HaloTag or IκB-HaloTag. To demonstrate that HaloTag can be successfully used to study different aspects of the NF-κB signaling pathway, we generated a vector encoding a p65-HaloTag fusion protein. HeLa cells were transiently transfected with this vector and labeled with the TMR ligand. In a majority of transfected cells, the p65-HaloTag fusion showed cytosolic localization with exclusion from the nucleus (Figure 2, panel a). Upon stimulation of the cells with TNF-α, the fusion protein translocated from the cytosol to the nucleus, reaching maximal nuclear accumulation within 25−30 min. After ~120 min, fluorescently labeled protein moved back to the cytosol (see Supplementary Video online for real time p65-HaloTag translocation). These kinetics are consistent with published data describing agonist-dependent p65 translocation (*18, 19*).

TNF-α-dependent translocation was also observed in HEK-293 cells stably expressing the p65-HaloTag fusion (Figure 2, panel b). The mechanism responsible for this translocation can be examined by pretreating the cells with specific inhibitors of the nuclear transport process. SN50 is a cell permeant peptide that inhibits nuclear translocation of p65/p50 heterodimers by competing for a nuclear localization sequence binding site of the nuclear import system (*19, 20*). Leptomycin B is a specific inhibitor of the Crm1p nuclear export system that is responsible for transport of p65 from the nucleus back to the cytosol (*18, 19*). SN50 had no apparent effect on p65-HaloTag distribution in nonstimulated cells but completely blocked its nuclear translocation in TNF-α-stimulated cells. In comparison, pretreatment with leptomycin B affected distribution of p65-HaloTag in both nonstimulated and stimulated cells. In nonstimulated cells, leptomycin B treatment led to nuclear accumulation of a small fraction of fluorescently labeled protein. In TNF-α-stimulated cells, the majority of the fluorescently labeled protein pool was translocated and remained in the nucleus (Figure 2, panel b). These data indicate that the movement of labeled p65-HaloTag in cells utilizes the Crm1p nuclear import/export pathway in agreement with the established mechanism for intrinsic p65 shuttling.

To show that labeling of the p65-HaloTag fusion was specific, HeLa cells labeled with the TMR ligand were lysed and proteins were resolved by SDS-PAGE. A dominant fluorescent protein band of the expected size was detected (Figure 2, panel c), along with a few minor bands of lower molecular weight. Because no fluorescently labeled proteins were evident in nontransfected cells, these minor bands are likely to be degradation products. Protein labeling was apparently completed within 15 min, as no further increase in fluorescence intensity of the bands was observed with longer incubation time (Figure 2, panel c, lane 3). Taken together these data demonstrate that the TMR ligand readily penetrates the cell membrane and labels the p65-HaloTag fusion protein with high specificity.

Control experiments have demonstrated that the TMR ligand has no effect on cellular ATP levels, suggesting lack of toxicity (Supplementary Figure 1). We have also shown that the ligand does not affect morphology for a variety of cell types, including HEK-293 (Figure 2, panel b; Figure 3, panel a), HeLa (Figure 2, panel a, ref 21), CHO, L-929, U2-OS (human osteosarcoma), and SHIN3 (human ovarian cancer cells) (unpublished data). Proper lineage differentiation has also been observed for human neural progenitor cells labeled with the TMR ligand (*22*).

Western blot analysis of the nuclear and cytosolic fractions using anti-p65 antibody confirmed the imaging data (Figure 2, panel d). In control cells ($t = 0$), the p65-HaloTag protein fusion was detected only in the cytosolic fraction. Exposure to TNF-α for 30 min led to sig-

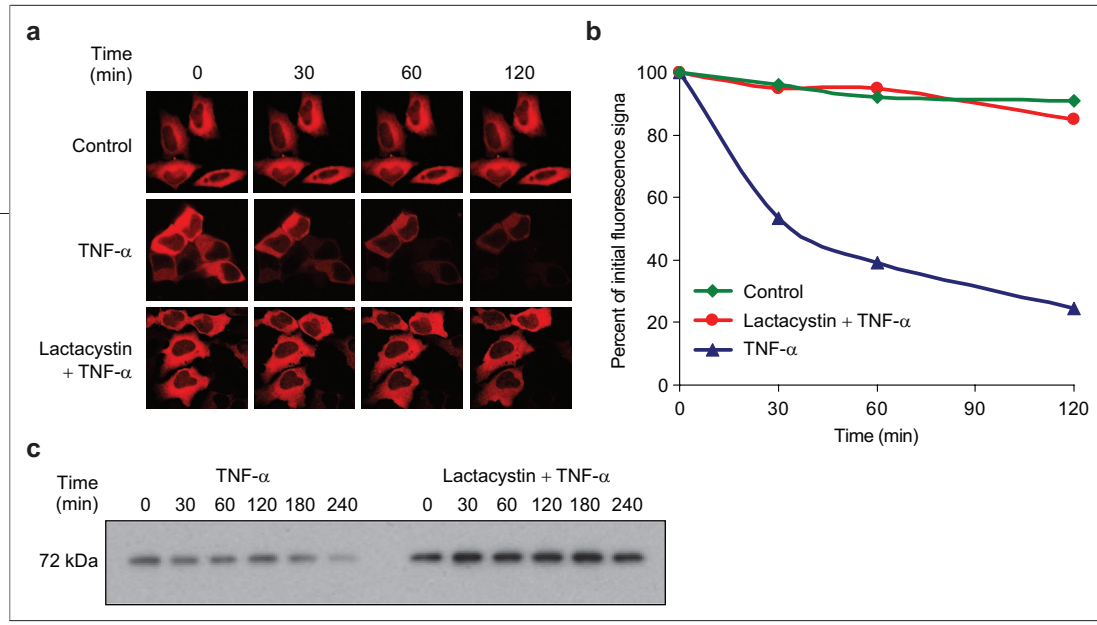

Figure 3. TNF-α-dependent degradation of IκBα-HaloTag fusion protein. a) Time series of images showing HEK-293 cells transiently expressing the IκBα-HaloTag fusion protein labeled with the TMR ligand (5 μM). Images were taken every 10 min for 3 h after addition of TNF-α (10 ng mL^{-1}) (images shown for 0, 30, 60, and 120 min after stimulation). Degradation was prevented by treatment of the cells with 10 μM lactacystin for 30 min prior to addition of TNF-α. b) Mean cellular fluorescence intensities were determined at each time point using FV500 software (Olympus) and plotted as a percentage of the initial fluorescence (t = 0 min.). c) Western blot analysis of IκB-HaloTag fusion protein degradation. Cells were treated with TNF-α (10 ng mL^{-1}) and harvested at the indicated times. Proteins were resolved by SDS-PAGE and visualized using an anti-IκB antibody.

nificant reduction in the cytosolic level with corresponding accumulation in the nuclear fraction. By 120 min the trend reversed, with a reduction in the nuclear fraction and increase in the cytosolic fraction. In addition, consistent with the known degradation of IκB in response to TNF-α signaling (*18, 19*), the level of IκB changed in correlation with the nuclear translocation of p65-HaloTag (Figure 2, panel b).

This agonist-dependent degradation could be visualized using a vector encoding IκB-HaloTag transiently transfected into HEK-293 cells. As expected, TNF-α produced a time-dependent reduction of total TMR fluorescence in the cells, declining 5-fold over 2 h (Figure 3, panels a and b). It is not surprising that some IκB-HaloTag remains throughout the experiment since the level of IκB-HaloTag is significantly higher than the intrinsic IκB. The reduction of fluorescence was blocked in the presence of lactacystin, an irreversible inhibitor of the S26 proteasome (*23*). Additional evidence for this inhibition was provided by Western blot analysis (Figure 3, panel c). These results are consistent with the suggestion that IκB degradation is carried out by the S26 proteasome (*15, 24*).

Interaction of p65-HaloTag with the IκB Promoter and IκB Protein. Formaldehyde cross-linking was used to demonstrate the interaction of p65-HaloTag with the IκB promoter, both within mammalian cells (Figure 4, panels a.i and a.ii) and in solution (Figure 4, panel a.iii). The intracellular interaction was measurable using p65-HaloTag expressed stably in HEK-293 cells or transiently in HeLa cells. Applying a chromatin capture protocol developed for the HaloLink Resin (see Methods), isolated DNA fragments cross-linked to the p65-HaloTag were amplified by PCR, revealing specific capture of the IκB promoter relative to the control (Figure 4, panel a.i and a.ii). This interaction was confirmed using p65-HaloTag expressed *in vitro* and cross-linked to purified genomic HeLa DNA (Figure 4, panel a.iii).

After stimulation with TNF-α, binding of p65-HaloTag to the IκB promoter increased by 6.8-fold in the stably transfected HEK-293 cells and by 3.5-fold in the transiently transfected HeLa cells. These values are comparable to results obtained for endogenous p65 protein using the chromatin immunoprecipitation (ChIP) assay (*25*). The increased binding correlates with the translocation of p65-HaloTag to the nucleus upon TNF-α stimulation (Figure 2). Absent stimulation, significant capture of the IκB promoter was still evident (Figure 4, panel a.ii, lane 1), possibly caused by heterogeneity within the cell population. This is common after transient transfections, as revealed by image analysis showing p65-HaloTag present within the nucleus of some cells prior to treatment with TNF-α (see Supplementary Video). This was not observed in the stably transfected cells (Figure 4, panel a.i, lane 1), which have equilibrated and have a lower expression level of p65-HaloTag.

A temporal profile of the interaction can be obtained by capturing DNA complexes with p65-HaloTag at various times following stimulation. This revealed maximal binding to the IκB promoter occurring ~30 min after ad-

dition of TNF-α (Figure 4, panel b.i). Protein complexes with p65-HaloTag can also be captured and analyzed by an analogous method omitting the cross-linking with formaldehyde. Using the same HEK-293 cells stably expressing p65-HaloTag, protein complexes were captured onto the HaloLink Resin and probed with an anti-IκB antibody (Figure 4, panel b.ii). This revealed that co-capture of the IκB protein was minimal at 30 min.

The interactions of p65-HaloTag with chromatin DNA and other proteins correlate to its movement from the cytosol to the nucleus, as revealed by the cellular imaging data. Taken together, the data are consistent with reduced interaction between p65 and IκB upon stimulation with TNF-α, caused by proteasome degradation of the IκB protein. The p65 then moves to the nucleus to bind to the IκB promoter, increasing expression of IκB, which re-establishes the interaction with p65 causing it to move back to the cytosol.

Genetically encoded fusion tags have broadly facilitated the study of biochemical and cellular phenomena by imparting useful properties onto their fusion partners. These properties include easily identifiable phenotypes such as fluorescence or luminescence, or affinity markers such as epitope tags. However, because each fusion tag normally embodies only a single property, we developed HaloTag to allow efficient interchangeability of tag properties. This was achieved by modifying the natural enzymatic reaction of haloalkane dehalogenase to enable specific and rapid covalent attachment of synthetic ligands onto the protein tag, either in solution or within cells. While in principle other hydrolytic enzymes could be similarly modified, haloalkane dehalogenase provides several advantages: the protein is small and absent in higher animals and plants (*26*), and the enzymatic reaction requires no cofactors or post-translational modifications. Moreover, the ligands can be designed to readily permeate cell membranes, be nontoxic and exhibit negligible cross-reactivity with other cellular proteins. Although the chloroalkane linker is structurally simple, it contains all of the essential features necessary for covalent binding and thus may be productively appended onto a broad variety of synthetic molecules. Accordingly, although we have demonstrated utility for general functionalities such as fluorophores and solid supports, other more specialized detection molecules and surfaces can be contemplated (*27*).

The chloroalkane linker forms an ester bond to Asp^{106} buried deeply within a hydrophobic pocket (*16*).

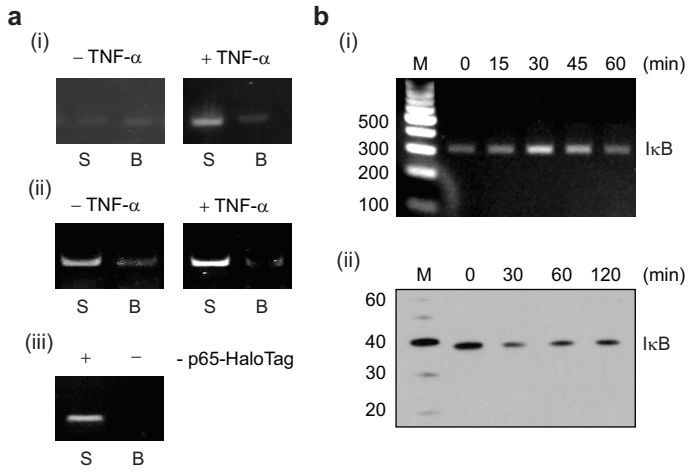

Figure 4. a) Covalent capture of IκB promoter by cross-linking to p65-HaloTag. Binding of p65-HaloTag to the IκB promoter was stimulated in stably transfected HEK-293 cells (i) or transiently transfected HeLa cells (ii), with TNF-α (20 ng mL^{-1}) for 30 min. Cells were then cross-linked with 1% formaldehyde, lysed, and sonicated, and p65-HaloTag:DNA complexes were captured on HaloLink Resin. *In vitro* expressed p65-HaloTag (iii) was isolated on HaloLink Resin, then cross-linked with formaldehyde to isolated HeLa genomic DNA. Experimental controls were established by splitting the sample and incubating one-half with the TMR ligand (i, ii) or using HaloLink Resin alone without p65-HaloTag (iii). DNA fragments were released by reversing the formaldehyde cross-links and purified, and the IκB promoter fragment (300 bp) was amplified by PCR. The PCR products, designated as signal (S) for the experimental samples and background (B) for the control samples, were resolved by 2% agarose gel and stained with ethidium bromide. b) p65-HaloTag binding to the IκB promoter and interaction with IκB protein are inversely correlated. (i) HEK-293 cells stably expressing p65-HaloTag were treated with TNF-α (20 ng mL^{-1}) and harvested at the indicated times. Capture of p65-HaloTag: DNA complexes and sample processing were performed as described in panel a. Maximum binding to the IκB promoter was observed at 30 min after stimulation. Sizes (bp) of DNA markers (M) are shown. (ii) IκB (38 kDa) bound to p65-HaloTag is revealed by co-capture on HaloLink Resin from stably expressing HEK-293 cells. Cells were treated with TNF-α (20 ng mL^{-1}) for the indicated times, lysed, incubated with HaloLink Resin, and washed to remove nonspecific interactions. Samples harvested at various times were resolved by 4–12% SDS-PAGE, transferred onto nitrocellulose, and visualized using an anti-IκB antibody. Minimum binding to IκB was observed at 30 min after treatment with TNF-α. Sizes (kDa) of protein markers (M) are shown.

The bond is relatively stable under conditions expected to disrupt protein structure, such as boiling in SDS. No significant loss of the fluorophore was evident following treatment for up to 20 min with SDS at 95 °C (data not shown). The bond is also apparently resistant to intracellular esterases, possibly due to the protective pocket. Correspondingly, disruption of this pocket upon protein degradation within cells could lead to bond hydrolysis.

The stability of this bond can provide several advantages relative to comparable affinity-based tags (*9*). First, tagged proteins may be imaged in living cells over extended periods without concern for dissociation of the label. Second, tagged proteins can also be visualized in chemically fixed cells, allowing for multiplexing with immunocytochemical methods (*21*). Third, tagged proteins can be visualized under standard protein analysis techniques such as SDS-PAGE and Western blot analysis, allowing for analysis of posttranslational protein modification. Finally, tagged protein can be rapidly immobilized on solid supports, such as agarose beads, and subjected to stringent wash conditions (*25*).

The ability to selectively attach alternative ligands onto HaloTag allows different analytical methods to be coordinated into a broader research strategy, without having to create new genetic constructs for each analysis. This can be particularly useful for stable transgenic cells, where reproducibly integrating different transgenes into the host cells is generally not feasible. In the presented example, image analysis of p65 behavior within living cells was correlated to biochemical analysis of protein and DNA interactions. By labeling the p65-HaloTag fusion with the TMR ligand, the time course of intracellular redistribution between the cytosol and nucleus could be examined under a variety of conditions. Capturing the same p65-HaloTag fusion onto agarose beads allowed co-capture of DNA fragments or other proteins bound to p65, which in turn allowed temporal analysis of these molecular interactions. The combined data thus allows direct correlation of the molecular interactions with intracellular localization.

Caution should be exercised when using fusion tags, as they have been known to interfere with biological processes under some circumstances (*3, 28, 29*). Fusions of p65 or IκB to HaloTag apparently did not interfere with normal protein function, as the fusion partners still exhibited the expected interactions with other proteins and DNA and showed proper localization and degradation within the cells. We further observed that the level of IκB was elevated in unstimulated cells expressing p65-HaloTag. Thus p65-HaloTag appears also to retain transcriptional activity, since IκB is under transcriptional control of p65/p50 heterodimer (*15*) and accordingly should be elevated by the presence of the fusion protein. Other examples of proteins fused to HaloTag have been recently published demonstrating appropriate cellular physiology, *e.g.*, voltage-gated K^+ channel (hERG/*KCNH2*) (*30*), X-linked inhibitor of apoptosis (XIAP)-associated factor 1 (*31*), and human β1integrin (*32*).

HaloTag activity is sufficiently retained following treatment with formaldehyde to support efficient capture of cross-linked protein−DNA complexes. This significantly provides a contiguous covalent chain linking the DNA fragments to the solid support, thus allowing highly stringent washing conditions for removing nonspecifically bound proteins and nucleic acids. This DNA capture method is simple and sensitive, and it avoids the burden associated with obtaining reliable antibodies necessary for chromatin immunoprecipitation (ChIP).

The data presented here provide a clear demonstration that HaloTag can be utilized to study cellular signaling with minimal deleterious effects on the proteins regulating these processes. Due to the interchangeable design of the ligands, the protein tag can be adapted to differing experimental requirements without altering the underlying genetic construct. Moreover, specialized techniques can be applied using differently colored fluorophores to selectively label proteins at different locations or synthesized at different times within the cell (unpublished data). The synthetic chemistry associated with the ligands enables their multifunctional nature, allowing additions of various functional groups and the ability to easily expand the capabilities of the technology in the future.

METHODS

See Supporting Information for detailed information about materials and the methods related to chemical synthesis of HaloTag ligands and resin, mutagenesis of the HaloTag protein, and protein purification and characterization.

Mammalian Cell Culture, Labeling with TMR Ligand, and Drug Treatment. HeLa (ATCC CCL-2) or HEK-293 (ATCC CRL-1573) cells were maintained in DMEM/F12 media supplemented with 10% FBS at 37 °C and 5% CO_2. For transient protein expression, cells were plated on 8-well Lab-Tek II chamber cover glass (Nunc) or 24-well plates at seeded density of $20-30 \times 10^3$ cells cm^{-2} and allowed to grow to ~85% confluency (~24−48 h). Cells were transfected using LT1 transfection reagent (Mirus Bio). The HEK-293 cells stably expressing fusion protein were generated using a vector co-transfection strategy.

For cell labeling, growth media was replaced with growth media containing the TMR ligand (5 μM). After 15 min, cells were rinsed twice with PBS (pH 7.4, 0.5 mL cm^{-2}) and incubated in fresh media for 30 min. The media was then replaced with fresh media or PBS, and the cells were used for imaging.

For TNF-α stimulation, cells expressing the p65-HaloTag or IκB-HaloTag fusion protein were serum-starved for 4 h and

treated by the addition of TNF-α to the media for 15−120 min at 37 °C and 5% CO_2. In some experiments, media-starved cells were pretreated with leptomycin B, SN50, or lactacystin.

Imaging of HaloTag Protein Fusions in Mammalian Cells. Live cells were imaged on an inverted confocal microscope FV500 (Olympus, Japan) using a 543 nm Ar/Kr laser line and filter set for TMR or transmitted light. Scanning speed and laser intensity were adjusted to avoid photobleaching of the fluorophores and damage to the cells. The microscope was equipped with a microenvironmental chamber to maintain physiological conditions during long-term experiments.

Western Blot Analysis. Cytosolic and nuclear fractions of cells were separated according to ref 33. Proteins were resolved by SDS-PAGE, probed with an anti-p65 antibody or anti-IκB antibody (both from BD, Biosciences), and visualized using the enhanced chemiluminescence (ECL) system (GE Healthcare).

Detection of HaloTag Fusion Proteins Using SDS-PAGE and Fluorimaging. Cells expressing the HaloTag fusion proteins and labeled with the TMR ligand were solubilized in SDS gel loading buffer (1% SDS, 10% glycerol, 1.0 mM β-mercaptoethanol, pH 6.8), boiled for 5 min, and resolved by SDS-PAGE. Gels were analyzed on a fluorescence imager Typhoon 9400 (GE Healthcare) at an Ex/Em appropriate for TMR (545/575 nm) or FAM (490/520 nm), processed for Western analysis, or stained with Coomassie Blue (Promega). Quantitation of bands was performed using ImageQuant (GE Healthcare).

Preparation of HaloLink Resin and Co-capture of IκB. The HaloLink Resin (100 μL) was centrifuged for 1 min at 3,000 rpm to remove ethanol and washed 3 times with 400 μL of TE pH 8.0 + 0.1% IGEPAL (Sigma).

Stable p65-HaloTag HEK-293 cells (1×10^6) were grown to 80% confluency, washed twice with PBS, and lysed with cytoplasmic lysis buffer (320 mM sucrose, 10 mM HEPES (pH 7.0), 5 mM $MgCl_2$). Cell lysates were incubated with prepared HaloLink Resin for 1 h at 22 °C, washed 3 times with 1.0 mL of TBS and resuspended in 20 μL of SDS gel loading buffer. Samples were heated to 95 °C for 5 min, resolved by 4−12% SDS-PAGE, and analyzed by Western blot using anti-IκB antibody (BD Biosciences).

Intracellular Formaldehyde Cross-Linking and PCR Analysis. HEK-293 cells (4×10^5) stably expressing or HeLa cells (4×10^5) transiently expressing the p65-HaloTag fusion protein were cross-linked for 10 min at 22 °C with 0.75% and then quenched by addition of 125 mM glycine (pH 7.0) to the media. Cells were washed twice with PBS, scraped, and pelleted at 5,000 rpm for 5 min. Lysis was performed using HaloCHIP lysis buffer (Promega), and chromatin was sheared using a Misonix 3000 sonicator with the Microtip 418 (power setting 2.5, with 12 cycles of 10 s pulse and 10 s rest on ice). Cell debris was removed by centrifugation at 12,000 rpm for 10 min at 4 °C.

Lysates were split into two tubes, labeled experimental and control. The control sample was incubated with HaloCHIP blocking ligand (Promega) for 30 min at 22 °C. Both samples were then incubated with HaloLink Resin for 2 h at 22 °C. Resin was washed in the following sequence: HaloCHIP lysis buffer, nuclease-free water (2×), HaloCHIP high salt wash (Promega), and nuclease free water (3×). The resin was resuspended in HaloCHIP reversal buffer (Promega) and incubated between 4 and 18 h at 65 °C. Released DNA was purified by PCR Clean-up kit (Qiagen). GoTaq Green Master Mix (Promega) was used for PCR: 2 min at 95 °C; 32 cycles of 95 °C for 1 min, 60 °C for 1 min, and 72 °C for 1 min; and extension at 72 °C for 5 min. The human IκB promoter PCR primers were 5′-GACGACCCCAATTCAAATCG-3′ and 5′-TCAGGCTCGGGGAATTTCC-3′.

***In Vitro* Expression and Formaldehyde Cross-Linking.** P65-HaloTag was expressed using the TnT T7 Quick Coupled Transcription/Translation *in vitro* expression system (Promega). Reactions were incubated with HaloLink Resin and washed according to manufacturer's recommendations (Promega). HeLa Genomic DNA (100 ng) was incubated with HaloLink Resin for 30 min. Cross-linking, quenching, capture on HaloLInk Resin, reversal, and DNA purification were performed as described above.

Supporting Information Available: This material is available free of charge *via* the Internet.

REFERENCES

1. Giepmans, B. N. G., Adams, S. R., Ellisman, M. H., and Tsien, R. Y. (2006) The fluorescent toolbox for assessing protein location and function, *Science 312*, 217–224.
2. Kogure, T., Karasawa, S., Araki, T., Satio, K., Kinjo, M., and Miyawaki, A. (2006) A fluorescent variant of a protein from the stony coral *Montipora* facilitates dual-color single-laser fluorescence cross-correlation spectroscopy, *Nat. Biotechnol. 24*, 577–581.
3. Terpe, K. (2003) Overview of tag protein fusions: from molecular and biochemical fundamentals to commercial systems, *Appl. Microbiol. Biotechnol. 60*, 523–533.
4. Waugh, D. S. (2005) Making the most of affinity tags, *Trends Biotechnol. 23*, 316–320.
5. Marks, K. M., and Nolan, G. P. (2006) Chemical labeling strategies for cell biology, *Nat. Methods 3*, 591–596.
6. Chen, I., and Ting, A. (2005) Site-specific labeling of proteins with small molecules in live cells, *Curr. Opin. Biotechnol. 16*, 35–40.
7. Gronemeyer, T., Godin, G., and Johnsson, K. (2005) Adding value to fusion proteins through covalent labeling, *Curr. Opin. Biotechnol. 16*, 453–458.
8. Miller, L. W., and Cornish, V. W. (2005) Selective chemical labeling of proteins in living cells, *Curr. Opin. Chem. Biol. 9*, 1–6.
9. Miller, L. W., Cai, Y., Sheetz, M. P., and Cornish, V. W. (2005) *In vivo* protein labeling with trimethoprim conjugates: a flexible chemical tag, *Nat. Methods 2*, 255–257.
10. Adams, S. R., Campbell, R. E., Gross, L. A., Martin, B. R., Walkup, G. K., Yao, Y., Llopis, J., and Tsien, R. Y. (2002) New biarsenical ligands and tetracystein motifs for protein labeling *in vitro* and *in vivo*: Synthesis and biological applications, *J. Am. Chem. Soc. 124*, 6063–6076.
11. Martin, B. R., Giepmans, B. N. G., Adams, S. R., and Tsien, R. Y. (2005) Mammalian cell-based optimization of the biarsenical-binding tetracysteine motif for improved fluorescence and affinity, *Nat. Biotechnol. 23*, 1308–1314.
12. Keppler, A., Gendreizing, S., Gronemeyer, T., Pick, H., Vogel, H., and Johnsson, K. (2003) A general method for the covalent labeling of fusion proteins with small molecules in vivo, *Nat. Biotechnol. 21*, 86–89.
13. Janssen, D. B. (2004) Evolving haloalkane dehalogenase, *Curr. Opin. Chem. Biol. 8*, 150–159.
14. Pries, F., Kingma, G. H., Jeronimus-Stratingh, C. M., Bruins, A. P., and Janssen, D. B. (1995) Histidine 289 is essential for hydrolysis of the alkyl-enzyme intermediate of haloalkane dehalogenase, *J. Biol. Chem. 270*, 10405–10411.
15. Hoffmann, A., and Baltimore, D. (2006) Circuitry of nuclear factor kappaB signaling, *Immunol. Rev. 210*, 171–186.
16. Newman, J., Peat, T. S., Richard, R., Kan, L., Swanson, P. E., Affholter, J. A., Holmes, I. H., Schindeler, J. F., Unkefer, C. J., and Terwilliger, T. C. (1999) Haloalkane dehalogenases: structure of a *Rhodococcus* enzyme, *Biochemistry 38*, 16105–16114.
17. Qureshi, M. H., Yeung, J. C., Wu, S-C., and Wong, S-L. (2001) Development and characterization of a series of soluble tetrameric and monomeric streptavidin mutants with differential biotin binding affinities, *J. Biol. Chem. 276*, 46422–46428.

18. Schmid, J. A., Birbach, A., Hofer-Warbinek, R., Pengg, M., Burner, U., Furtmuller, P. G., Binder, B. R., and de Martin, R. (2000) Dynamics of NF κB and IκBα studied with green fluorescent protein (GFP) fusion proteins. Investigation of GFP-p65 binding to DNA by fluorescence resonance energy transfer, *J. Biol. Chem. 275*, 17035–17042.
19. Nelson, G., Paraoan, L., Spiller, D. G., Wilde, G. J., Browne, M. A., Djali, P. K., Unitt, J. F., Sullivan, E., Floettmann, E., and White, M. R. (2002) Multi-parameter analysis of the kinetics of NF-κB signalling and transcription in single living cells, *J. Cell. Sci. 115*, 1137–1148.
20. Lin, Y. Z., Yao, S. Y., Veach, R. A., Torgerson, T. R., and Hawiger, J. (1995) Inhibition of nuclear translocation of transcription factor NF-κB by a synthetic peptide containing a cell membrane-permeable motif and nuclear localization sequence, *J. Biol. Chem. 270*, 14255–14258.
21. Los, G. V., and Wood, K. V. (2006) The HaloTag: A novel technology for cell imaging and protein analysis. In *Methods in Molecular Biology – High Content Screening: A Powerful Approach to System Cell Biology and Drug Discovery* (Guliano, K. , Taylor, D. L., and Haskin, J., Eds.), pp 195−208, Humana Press, Inc., Totowa, NJ.
22. Behrstock, S., McMillan, E., Zimprich, C., Ebert, A., Tork, C., Svendsen, C., Los, G. (2007) A novel reporter protein fused to α-synuclein can be expressed in human neural cells for modeling disease in vitro and for tracking cells in vivo. *The Society for Neuroscience Annual Meeting,* November 4−11, 2007, San Diego, CA.
23. Fenteany, G., Standaert, R. F., Lane, W. S., Cho, S., Corey, E. J., and Schreiber, S. L. (1995) Inhibition of proteasome activities and subunit-specific amino-terminal threonine modification by lactacystin, *Science 268*, 726–731.
24. Chen, Z. J. (2005) Ubiquitin signaling in the NF-κB pathway, *Nat. Cell Biol. 7*, 758–765.
25. Nowak, D. E., Tian, B., and Brasier, A. R. (2005) Two-step cross-linking method for identification of NF-κB gene network by chromatin precipitation, *BioTechniques 39*, 715–725.
26. Naested, H., Fennema, M., Hao, L., Andersen, M., Janssen, D. B., and Mundy, J. (1999) A bacterial haloalkane dehalogenase gene as a negative selectable marker in Arabidopsis, *Plant J. 18*, 571–576.
27. Zhang, Y., So, M. K., Loening, A. M., Yao, H., Gambhir, S. S., and Rao, J. (2006) HaloTag protein-mediated site-specific conjugation of bioluminescent proteins to quantum dots, *Angew. Chem., Int. Ed. 45*, 4936–4940.
28. Agbulut, O., Coirault, C., Niederlander, N., Huet, A., Vicart, P., Hagege, A., Puceat, M., and Menasche, P. (2006) GFP expression in muscle cells impairs actin-myosin interactions: implications for cell therapy, *Nat. Methods 3*, 331.
29. Baens, M., Noels, H., Broeckx, V., Hagens, S., Fevery, S., Billiau, A. D., Vankelecom, H., and Marynen, P. (2006) The dark side of EGFP: defective polyubiquitination, *PLoS ONE 1*, e54.
30. Los, G., Anson, B., Zimprich, C., Karassina, N., January, C., and Bulleit, R. F. (2004) The HaloTag: A Novel Technology for Protein Labeling in Living Cells: Effect of the HaloTag TM System on hERG Channel Activity. In *FENS Forum 2004*, p 196, Federation of European Neuroscience Societies (FENS), Berlin.
31. Straszewski-Chavez, S., Visintin, I., Karassina, K., Los, G., Liston, P., Halaban, R., Fadiel, A., and Mor, G. (2007) XAF1 mediates tumor necrosis factor-α-induced apoptosis and X-linked inhibitor of apoptosis cleavage by acting through the mitochondrial pathway, *J. Biol. Chem. 282*, 13059–13072.
32. Svendsen, S., Zimprich, C., McDougall, M., Klaubert, D., and Los, G. (2008) Spatial separation and bidirectional trafficking of proteins using a multi-functional reporter, *BMC Cell Biol. 9*, 17.
33. Carlotti, F., Chapman, R., Dower, S. K., and Qwarnstrom, E. E. (1999) Activation of nuclear factor κB in single living cells. Dependence of nuclear translocation and anti-apoptotic function on EGFPRELA concentration, *J. Biol. Chem. 274*, 37941–37949.